Chemical Science

RSC Publishing

EDGE ARTICLE

View Article Online
View Journal | View Issue

A mechanistic study of proton reduction catalyzed by a pentapyridine cobalt complex: evidence for involvement of an anation-based pathway†

Cite this: *Chem. Sci.*, 2013, **4**, 1578

Amanda E. King,[a] Yogesh Surendranath,[a] Nicholas A. Piro,[ae] Julian P. Bigi,[ae] Jeffrey R. Long*[ad] and Christopher J. Chang*[abce]

The pentapyridine cobalt complex $[Co(PY5Me_2)]^{2+}$ and its congeners have been shown to catalyze proton reduction to hydrogen in aqueous solution over a wide pH range using electrical or solar energy input. Here, we employ electrochemical and spectroscopic studies to examine the mechanisms of proton reduction by this parent complex under soluble, diffusion-limited conditions in acetonitrile with acetic acid as the proton donor. Two pathways for proton reduction are identified *via* cyclic voltammetry: one pathway occurring from an acetonitrile-bound $Co^{II/I}$ couple and the other pathway operating from an acetate-bound $Co^{II/I}$ couple. Kinetics studies support protonation of a Co^{I} species as the rate-determining step for both processes, and additional electrochemical measurements further suggest that the onset of catalysis from the acetonitrile-bound $Co^{II/I}$ couple is highly affected by catalyst electronics. Taken together, this work not only establishes the $CoPY5Me_2$ unit as a unique molecular platform that catalyzes the reduction of protons under soluble, diffusion-limited conditions in both aqueous and organic media, but also highlights the participation of anation processes that are likely relevant for a wide range of hydrogen-producing and related catalytic systems.

Received 14th December 2012
Accepted 12th February 2013

DOI: 10.1039/c3sc22239j

www.rsc.org/chemicalscience

Introduction

The concomitant rise in global energy demands and growing concerns over climate change have led to increased interest in exploring alternative energy resources.[1] In this context, hydrogen has garnered considerable attention as a potential molecular fuel whose use could result in a closed, carbon-neutral energy production system.[2] In nature, both mono- and bimetallic hydrogenase enzymes mediate the equilibrium between H_2 and protons/electrons in aqueous media at the thermodynamic overpotential and with turnover frequencies as high as 10 000 per mole catalyst per second.[3] As such, the search for robust synthetic H_2 production systems that match the efficiency of hydrogenases has resulted in the design of a number of structural and functional mimics.[3,4] In this regard, inorganic model complexes of hydrogenase active sites have greatly contributed to our mechanistic understanding of these enzymes, but their common requirement for organic solvents, instability to air, and the need for strong acids has precluded their widespread use in functional device systems.[3] In addition, many elegant abiotic monometallic H_2 production systems have been developed; however, high reactivity at low overpotentials in aqueous media is largely restricted to the use of low-abundance and expensive precious metal centers,[5] whereas molecular proton reduction catalysts based on earth-abundant metals often require organic solvents or additives, strong acids, and/or relatively high overpotentials.[6,7] Notable elegant exceptions include tethered molecular catalysts that show tolerance to aqueous media,[7e,7j,8] as well as hydrogenase mimics that operate in aqueous media.[9] Thus, the invention of water-stable molecular catalysts for H_2 production using earth-abundant metals remains a significant challenge.

To meet this need, we have initiated a broad-based program to create earth-abundant metal catalyst platforms that can operate in clean aqueous media.[10] As part of these investigations, we recently reported the reactivity of a family of hydrogen catalysts supported by chelating polypyridine ligand frameworks (Chart 1).[11] The molybdenum(IV)-oxo catalyst employing 2,6-bis(1,1-bis(2-pyridyl)ethyl)pyridine ($PY5Me_2$) was shown to catalyze robust H_2 production in both seawater[11a] and acetonitrile solutions.[11b] The related molybdenum(IV) disulfide,

[a]*Departments of Chemistry, University of California, Berkeley, California 94720, USA. E-mail: chrischang@berkeley.edu; jrlong@berkeley.edu*

[b]*Departments of Molecular and Cell Biology, University of California, Berkeley, California 94720, USA*

[c]*Howard Hughes Medical Institute, University of California, Berkeley, California 94720, USA*

[d]*Materials Sciences Division, Lawrence Berkeley National Laboratory, Berkeley, California 94720, USA*

[e]*Chemical Sciences Division, Lawrence Berkeley National Laboratory, Berkeley, California 94720, USA*

† Electronic supplementary information (ESI) available. CCDC 915137, 915338, 915155 and 915156. For ESI and crystallographic data in CIF or other electronic format see DOI: 10.1039/c3sc22239j

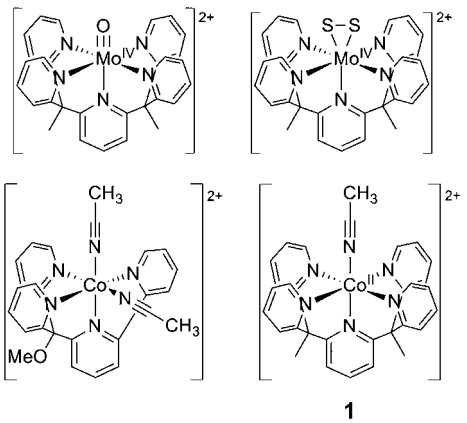

1

Chart 1 Water-compatible molecular polypyridine catalysts for proton reduction.

obtained by exposure of a molybdenum(II) $PY5Me_2$ precursor to elemental sulfur, is also capable of generating H_2 from acidic aqueous or organic media, and provides a structural and functional mimic for the triangular edge active sites of MoS_2.[11c] In first-row transition metal chemistry, we showed that a cobalt(II) complex ligated by 2-bis(2-pyridyl)(methoxy)methyl-6-pyridylpyridine (PY4) can effect catalytic proton reduction in 1 : 1 H_2O : MeCN mixtures,[11d] where the onset of catalysis occurred at the potential observed for the Co^{II}/Co^{I} redox couple. Finally, the complex $[Co(PY5Me_2)]^{2+}$ (**1**) displayed catalytic H_2 production in aqueous solutions at neutral pH with a turnover frequency of 300 mmol H_2 per mole catalyst per second at a 660 mV overpotential.[11e] Introduction of various functional groups in the *para* position of the central pyridine ring resulted in rational shifts for both the Co^{II}/Co^{I} reduction potential and onset of catalytic proton reduction; indeed, the least reducing derivative bearing a CF_3 functionality was capable of mediating both electro- and photocatalytic hydrogen production under diffusion-limited conditions in aqueous media at physiological pH.[12]

During our initial investigations of the $Co(PY5Me_2)$ platform, we noted that the catalytic activity of **1** in water is unusual compared to the activity of the vast majority of other well-studied cobalt(II) proton-reduction systems, in that the catalytic onset potential is not at the Co^{II}/Co^{I} couple but rather from a species with a more negative reduction potential.[9c,11e,13] Intrigued by this result, we sought to obtain more insight into the mechanisms of proton reduction by **1** by performing experiments under homogenous, diffusion-limited conditions that allow systematic control of acid strength and concentration. In this report, we present electrochemical and spectrophotometric studies on **1** in acetonitrile solution with acetic acid as the proton donor, showing that this platform is a competent hydrogen-producing electrocatalyst under soluble, diffusion-limited conditions in both organic and aqueous media. Interestingly, we observe two mechanistic pathways: one pathway occurring from an acetonitrile-bound $Co^{II/I}$ couple and the other pathway operating from an acetate-bound $Co^{II/I}$ couple. The identification of an anation-assisted pathway has broader implications for proton reduction catalysts, particularly in the design of systems with minimized overpotential under ionic aqueous media.

Results and discussion

Synthesis and characterization of $[Co(PY5Me_2)]^{n+}$ complexes

In the absence of a proton source in acetonitrile, the cyclic voltammogram of **1** exhibits two reversible redox processes (Fig. 1). The one-electron oxidation of **1** to form a $[Co^{III}(PY5Me_2)]^{3+}$ species (**2**) occurs at $E_{1/2}$ = 815 mV, while the one-electron reduction of **1** to furnish a $[Co^{I}(PY5Me_2)]^{+}$ species (**3**) occurs at $E_{1/2} = -830$ mV (all potentials reported herein are referenced to SHE).

The reversible nature of the redox processes observed for **1** suggested that the Co^{I} and Co^{III} congeners could be independently synthesized. Accordingly, exposure of **1** to $NOBF_4$ yields $[Co^{III}(NCMe)(PY5Me_2)]^{3+}$ (**2**) (Scheme 1). The UV-visible spectrum of **2** shows a weak absorption at 490 nm and a shoulder at 360 (Fig. S1†), and the diamagnetic ^1H NMR spectrum indicates a low-spin d^6 complex (Fig. S1†). Compound **2** proved amenable to structure determination using X-ray crystallographic techniques and displayed the six-coordinate octahedral geometry expected for a low-spin d^6 complex (Fig. 2). All Co–N bond distances contract upon oxidation of **1**, with the $Co–N_{axial}$ bond length showing the largest decrease from 2.09(6) Å to 1.93(6) Å and the $Co–N_{equatorial}$ bond distances decreasing from an average of 2.12(8) Å to 1.98(2) Å.[14] The 0.09(7) Å out-of-plane shift observed in **1** decreases to 0.00(1) Å in **2**.

Adding equimolar amounts of $Co(PPh_3)_3Cl$ to a benzene solution containing $PY5Me_2$ yields $[Co^{I}(PY5Me_2)]^{+}$ (**3**). Compound **3** also proved amenable to structure determination using single-crystal X-ray diffraction analysis (Fig. 2). Here, the complex adopts a square pyramidal geometry at the cobalt center, with an empty coordination site due to the synthesis and recrystallization in a weakly coordinating solvent. The contraction of the $Co–N_{axial}$ bond length in **3** to 1.96(8) Å and two trans $Co–N_{equatorial}$ bonds to 2.01(3) Å and 2.02(8) Å upon reduction results in the cobalt center residing in a 'saddle-shaped' environment. Additionally, **3** displayed a broad, paramagnetically shifted ^1H-NMR spectrum consistent with a high-spin d^8 electronic

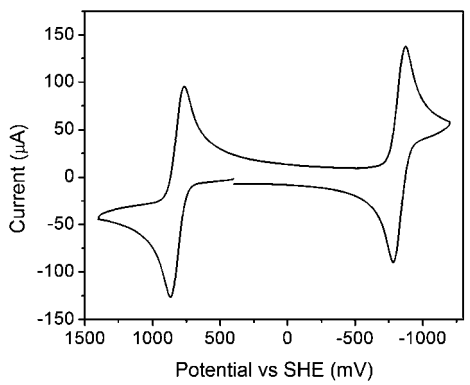

Fig. 1 Cyclic voltammogram of **1** in acetonitrile. Conditions: [**1**] = 10 mM, $[NBu_4PF_6]$ = 100 mM, working/auxiliary/reference electrodes = glassy carbon disk/Pt wire/silver wire, scan rate = 100 mV s^{-1}.

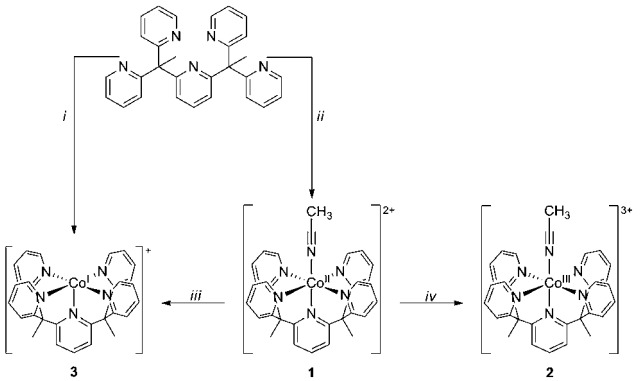

Scheme 1 Synthesis of compounds **1**, **2**, and **3**. Conditions: (i) metalation with one equivalent of $Co(PPh_3)_3Cl$ in toluene, followed by salt metathesis with $NaBPh_4$ in acetonitrile. (ii) Metalation with $Co(OTf)_2(MeCN)_2$ in acetonitrile. (iii) Reduction with one equivalent of KC_8 in THF. (iv) Oxidation with one equivalent of $NOBF_4$ in acetonitrile.

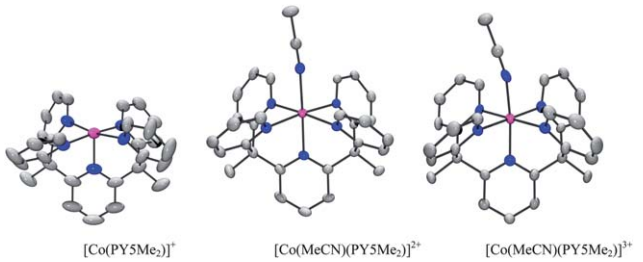

Fig. 2 Crystal structures of the cobalt complexes in **3** (left), **1** (center), and **2** (right). Ellipsoids are drawn at the 50% probability level, with purple, blue, and gray representing Co, N, and C atoms, respectively; H atoms are omitted for clarity.

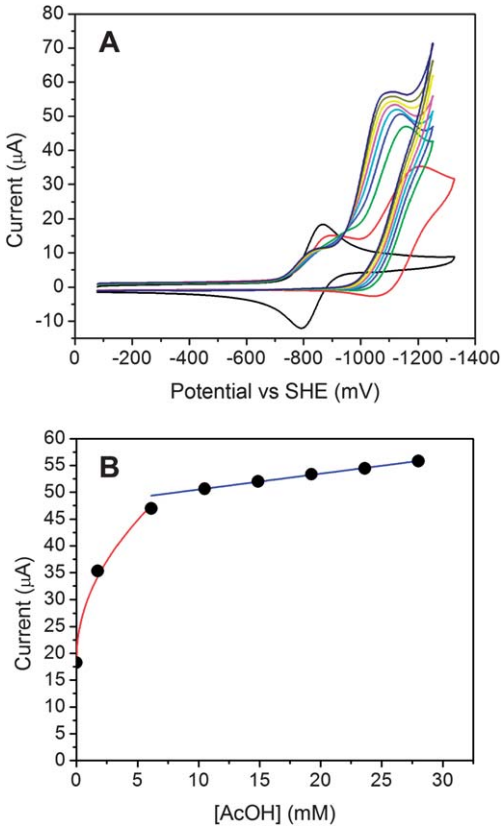

Fig. 3 Electrochemical behavior of **1** upon addition of catalytic amounts of acetic acid. Conditions for all plots: $[NBu_4PF_6]$ = 100 mM, working/auxiliary/reference electrodes = glassy carbon disk/Pt wire/silver wire, scan rate = 100 mV s^{-1}. (A) Cyclic voltammograms of **1** in the absence and presence of acetic acid in acetonitrile. Conditions: [**1**] = 1 mM, [AcOH] = 0–28 mM. (B) Plot of maximum current at *versus* [AcOH]. The red line reflects a fit to $y = mx^{1/2} + b$, while the blue line reflects a fit to $y = mx + b$.

structure; an $S = 1$ ground state was also indicated by DFT calculations, with the singlet state lying 16.6 kcal mol^{-1} above the triplet state. This difference in energy suggests that the singlet excited state may be accessible in reactions of **5** at 20 °C (Fig. S2†). In analogy to other isolated Co^{I} species in a tetragonal ligand framework,[15] **3** shows two broad absorption features centered at 650 and 825 nm in its UV-visible spectrum (Fig. S3†). Spectroelectrochemical measurements confirm that reduction of **1** yields **3** (Fig. S4†).

Catalytic reduction of protons from acetic acid in acetonitrile

The use of water as both a solvent and proton source, although desirable from a device compatibility and green chemistry perspective, can hamper detailed mechanistic studies because there is little control over proton delivery to the reduced catalyst. To address this issue, all kinetic studies were performed using acetonitrile as a solvent with acetic acid as a titratable proton source. Addition of acetic acid results in a simultaneous broadening and decrease in the current observed for the Co^{II}/Co^{I} redox process and the appearance of a new catalytic wave at −1100 mV, 270 mV more negative than the $E_{1/2}$ of the Co^{II}/Co^{I} couple (Fig. 3A). Furthermore, anodic scans reveal the development of a wave at 400 mV (Fig. S5†). The direct reduction of acetic acid in the absence of **1** occurs at −1400 mV, with negligible background current at the potentials where catalysis occurs. Gas chromatography data collected for samples taken from the bulk electrolysis cell headspace confirm that H_2 is generated at 100% Faradaic efficiency.

Plotting the current obtained at −1100 mV as a function of [**1**] suggests first- and zero-order dependences[16] at low and high acid concentrations, respectively (Fig. 3B). However, it is important to note that the peak-shaped nature of both new features indicate the involvement of competing processes, including substrate depletion (*vide infra*).

Deconvoluting the redox processes of 3 upon addition of acetic acid and identification of the catalyst resting state

The electrochemical behavior of **1** at low acid : catalyst ratios was examined to study further the catalytic processes observed upon addition acetic acid (Fig. 4A). Titration of stoichiometric amounts of acetic acid into an acetonitrile solution of **1** decreases the current observed at −830 mV and gives rise to a new process at −1100 mV. Scanning to potentials less negative than onset of the process at −1100 mV does not restore the reversibility of the Co^{II}/Co^{I} redox couple (Fig. S6†). Furthermore,

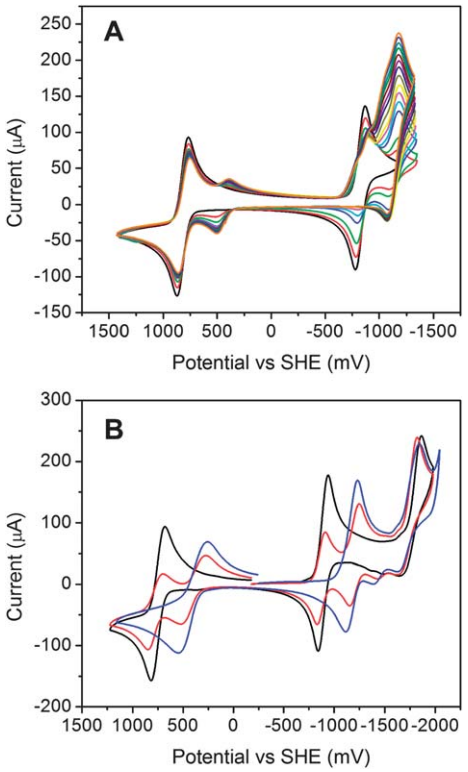

Fig. 4 Cyclic voltammograms of **1** upon addition of stoichiometric amounts of acetic acid and tetrabutylammonium acetate. Conditions for all plots: $[NBu_4PF_6]$ = 100 mM. Working/auxiliary/reference electrodes = glassy carbon disk/Pt wire/silver wire. Scan rate of 100 mV s^{-1}. (A) Cyclic voltammograms of **1** in the absence and presence of acetic acid in acetonitrile. The second scan is shown. Conditions: [**1**] = 10 mM, [AcOH] = 0–10 mM. (B) Cyclic voltammograms of **3** in the absence and presence of tetrabutylammonium acetate in acetonitrile. Conditions: [**1**] = 10 mM, $[NBu_4OAc]$ = 0 (black), 5 (red), or 10 (blue) mM.

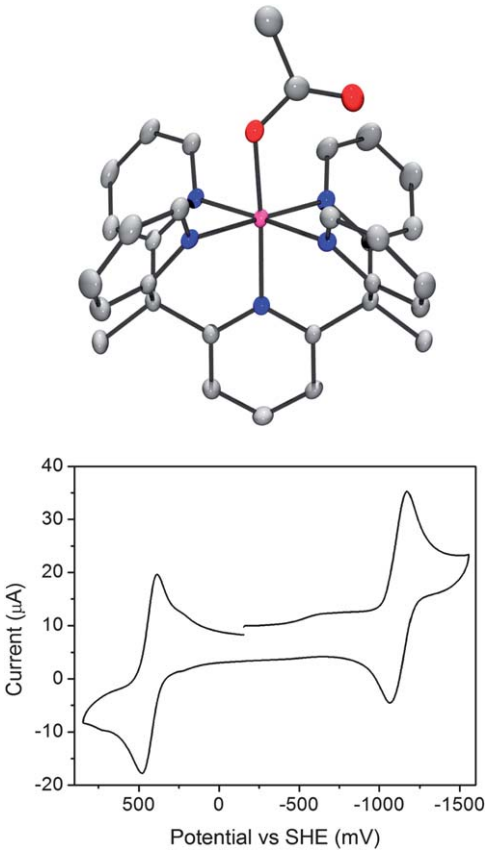

Fig. 5 Structure and electrochemical behavior of **4**. Conditions for cyclic voltammetry: $[NBu_4PF_6]$ = 100 mM, working/auxiliary/reference electrodes = glassy carbon disk/Pt wire/silver wire.

the redox process that develops at $E_{1/2}$ = 400 mV is once again only observed after a cathodic scan.

We hypothesized that a possible chemical origin for the wave observed at $E_{1/2}$ = 400 mV is the anation of acetate to form an acetate-bound $[Co(PY5Me_2)(OAc)]^+$ species. To test this idea, titration a solution of **1** with tetrabutylammonium acetate results in not only the formation of a wave at $E_{1/2}$ = 400 mV but also the formation of the wave at $E_{1/2}$ = −1180 mV (Fig. 4B). The independent synthesis of $[Co(PY5Me_2)(OAc)]^{2+}$ (**4**) and its subsequent examination by cyclic voltammetry further confirmed that the new processes at 400 mV and −1100 mV observed in Fig. 4A are indeed due to the $Co^{III}(OAc)/Co^{II}(OAc)$ and $Co^{II}(OAc)/Co^{I}(OAc)$ couples, respectively (Fig. 5). The observed shifts in the oxidation and reduction potentials upon coordination of acetate can be understood in terms of the change of the overall charge on the cobalt complex, with the more negatively charged cobalt center being more difficult to reduce and easier to oxidize. Additionally, acetate binds readily to **1**, with no evidence for the acetonitrile-bound cation observed in the cyclic voltammogram of a 1 : 1 **1**–NBu_4OAc mixture.

The observation of a $Co^{III}(OAc)/Co^{II}(OAc)$ couple only after a reductive scan is performed in the presence of acetic acid suggests that the equilibrium shown in eqn (1) favors the reactants. This behavior can be rationalized by the relatively high pK_a of acetic acid in acetonitrile, which favors the formation of acetic acid over an acetate-bound cobalt species and a free proton in solution.

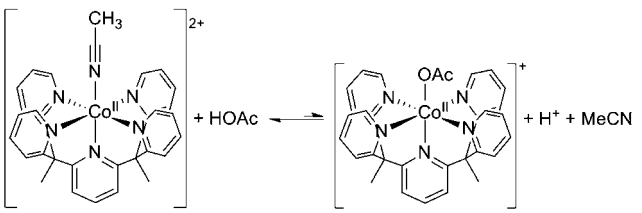

(1)

To verify this hypothesis, the titration of **1** with both acetic acid and tetrabutylammonium acetate was observed spectrophotometrically. Whereas addition of catalytically relevant concentrations of acetic acid does not lead to spectral changes, addition of tetrabutylammonium acetate results in the appearance of a new charge-transfer band at 550 nm (Fig. 6). The observation of redox processes due to both the Co^{II}/Co^{I} and $Co^{II}(OAc)/Co^{I}(OAc)$ couples indicates that the resting state of the catalyst is highly dependent on the presence of acetate. The UV-visible spectra shown in Fig. 6 indicate that the resting state of the catalyst with acetic acid is an acetonitrile-bound cobalt

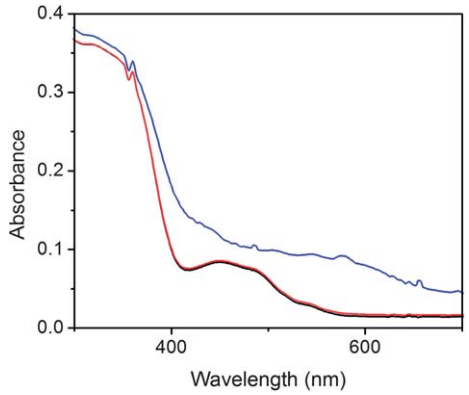

Fig. 6 Spectrophotometric characterization of **1** in acetonitrile (5 mM) with various acetate sources. (A) UV-visible spectrum of **1** (black), **1** with 40 equivalents of acetic acid (red), and **1** with one equivalent of Bu_4NOAc (blue).

center. However, both UV-visible spectra and cyclic voltammetry data indicate that, upon the addition of acetate as either intentionally or as the result of acetic acid reduction, the identity of the catalyst is best described as an acetate-ligated species.

Catalysis under conditions with added acetate

To further investigate the catalytic behavior observed from the $Co^{II}(OAc)/Co^{I}(OAc)$ couple, two different conditions were examined. In the first modification, a 1 : 1 mixture of acetic acid–tetrabutylammonium acetate was titrated into a solution of **1** (Fig. 7A). A single catalytic wave develops at the potential associated with the $Co^{II}(OAc)/Co^{I}(OAc)$ couple. Kinetic studies revealed a first-order dependence on [AcOH/Bu_4NOAc] under these conditions (Fig. 7B). As observed for conditions in which only acetic acid is used, gas chromatographic analysis of the bulk electrolysis cell headspace confirms that H_2 is generated at 100% Faradaic efficiency.

In the second set of conditions, the effect of acetic acid on a solution of 1 : 1 mixture of **1**–tetrabutylammonium acetate was examined. A single catalytic wave develops at the potential associated with the $Co^{II}(OAc)/Co^{I}(OAc)$ couple, with the peak current moving to more positive potentials with increasing acid concentration (Fig. 8A). Additionally, a first-order dependence is observed in [AcOH] (Fig. 8B). As predicted by the UV-visible spectra shown in Fig. 6B, the catalyst remains ligated by acetate; catalysis from an acetonitrile-bound $Co^{II/I}$ couple is not observed. Additionally, titration of tetrabutylammonium acetate into a solution of $[Co(PY5Me_2)(OAc)]^+$ with catalytic amounts of acetic acid results in not only the shift of the observed peak current to more negative potentials (Fig. 9A) but also the decrease of the observed peak current (Fig. 9B), thus suggesting an inhibitory effect of acetate on catalysis.

Taking all collective data into account, the initial mechanism for proton reduction with acetic acid as the proton source likely involves the protonation of the acetonitrile-bound Co^{I} species, as evidenced in the broadening of the feature at −830 mV shown in Fig. 3 (eqn (2)). This feature does not grow appreciably, however, because the acetate that is necessarily formed during this initial

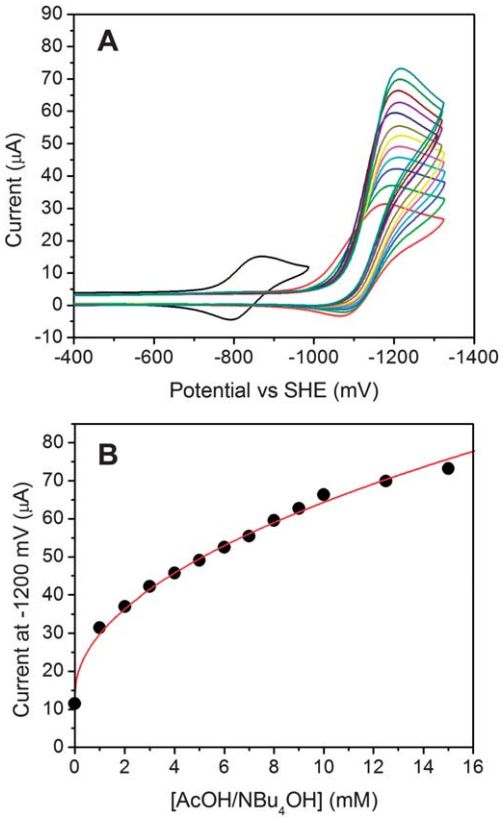

Fig. 7 Cyclic voltammograms of **1** upon addition of catalytic amounts of a 1 : 1 acetic acid–NBu_4OAc mixture. Conditions for all plots: [NBu_4PF_6] = 100 mM, working/auxiliary/reference electrodes = glassy carbon disk/Pt wire/silver wire, scan rate = 100 mV s^{-1}. (A) Cyclic voltammograms of **1** in the absence and presence of acetic acid in acetonitrile. Conditions: [**1**] = 1.0 mM, [AcOH] = 0–15 mM. (B) Plot of current at −1200 mV *versus* [AcOH].

catalysis will result in the formation of an acetate-ligated species that displays both redox and catalytic activity at more negative potentials than the parent complex (eqn (3)). The build-up and coordination of acetate to **1** during catalysis results in both the decrease in current observed for the acetonitrile-bound Co^{II}/Co^{I} during the initial portions of the cyclic voltammetry scan and the development of the feature observed at $E_{1/2} = -1180$ mV.

$$Co^{I} + HOAc \rightarrow Co^{II} + \tfrac{1}{2}\, H_2 + OAc^- \quad (2)$$

$$Co^{II} + OAc^- \rightarrow Co^{II}OAc \quad (3)$$

In this context, a common feature amongst the majority of reported cobalt catalysts for aqueous or aqueous-compatible proton reduction is the development of a catalytic current at the $Co^{II/I}$ couple.[11d,13,15] The notable exceptions to this observation include the $PY5Me_2$ systems discussed in this study, a tetraazacyclotetradecadiene and two diglyoximate cobalt species reported by Peters,[9c] and a cobalt bis(iminopyridine) catalyst by Gray and Peters.[17] The cyclic voltammograms of these systems retain the redox feature associated with proton reduction, albeit with development of some catalytic activity at the $Co^{II/I}$ couple and subsequent loss of reversibility. Furthermore, a second, much larger catalytic wave develops at more negative potentials.

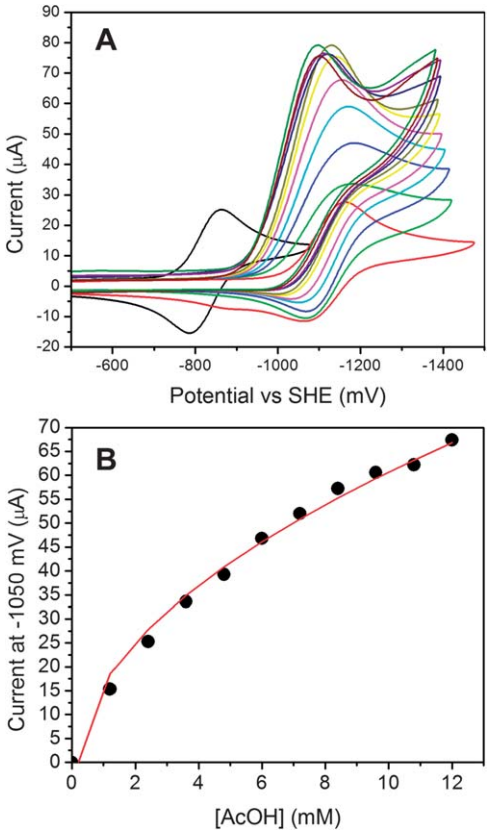

Fig. 8 Cyclic voltammograms of a 1 : 1 mixture of **1**–NBu_4OAc upon addition of catalytic amounts of acetic acid. Conditions: $[NBu_4PF_6]$ = 100 mM, working/auxiliary/reference electrodes = glassy carbon disk/Pt wire/silver wire, scan rate = 100 mV s^{-1}. (A) Cyclic voltammograms of **3** in the absence and presence of acetic acid in acetonitrile. Conditions: [**1**] = 1.0 mM, [AcOH] = 0–12 mM. (B) Plot of current at −1050 mV *versus* [AcOH].

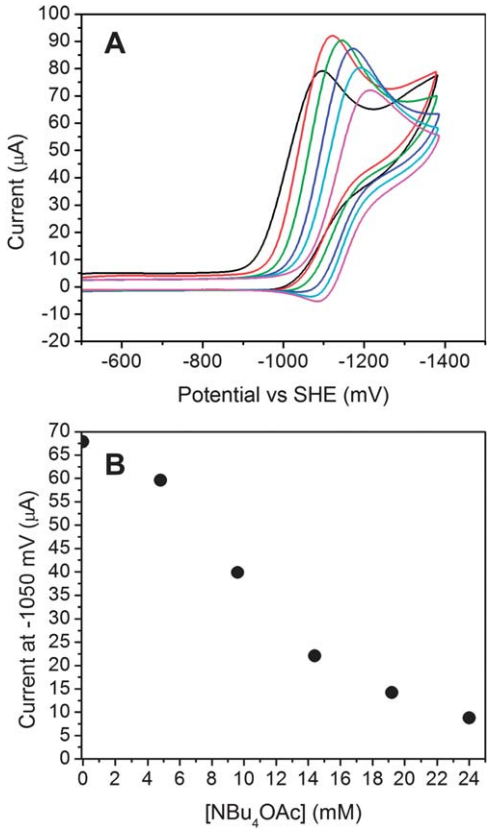

Fig. 9 Cyclic voltammetry of a 1 : 1 : 12 mixture of **1**–NBu_4OAc–AcOH upon addition of additional Bu_4NOAc. Initial conditions: $[NBu_4PF_6]$ = 100 mM, [**1**] = $[NBu_4OAc]$ = 1.0 mM, [AcOH] = 12 mM. Working/auxiliary/reference electrodes = glassy carbon disk/Pt wire/silver wire. Scan rate = 100 mV s^{-1}. (A) Cyclic voltammograms of **1** obtained upon the addition of additional NBu_4OAc. Conditions: $[NBu_4OAc]$ = 0–24 mM. (B) Plot of current at −1050 mV *versus* $[NBu_4OAc]$.

In the cobalt bis(iminopyridine) system, this second feature is ascribed as occurring from a ligand-based reduction. In contrast, the second feature in the $[Co(PY5Me_2)]^{2+}$ systems is due to catalysis from an anion-ligated species. The observation of catalytic activity at the $Co^{II}(OAc)/Co^{I}(OAc)$ redox couple suggests that catalysis can occur from a six-coordinate Co^{I} species. Homogeneous catalysis from a six-coordinate tris-(glyoximato) Co^{II} chlathrochelate species had been proposed previously;[18] however Saveant demonstrated that both the propagation of a peak-shaped wave and the asymptotic rise to a limiting current even at high acid concentrations indicated that catalysis was occurring from cobalt nanoparticles deposited on the electrode surface during catalysis.[19] The cyclic voltammograms shown in Fig. 7A and 8A do not display the behavior reported for the six-coordinate tris(glyoximato) Co^{II} chlathrochelate species upon the addition acid, specifically with regards to the continued rise in current at increasing acid concentrations and the linear dependence between of the current *vs.* square root of scan rate (Fig. S7†). A likely mechanism for catalysis from an acetate-bound cobalt species is the protonation and subsequent dissociation of the acetate moiety from a cobalt(I) center, followed by rapid formation of a Co^{III}-hydride. Thus, the mechanism operative in H_2 evolution would then be expected to mirror the mechanism operative when anation is not a contributing factor (*vide infra*).

Effect of catalyst electronics and acid strength

Because the current enhancement at potentials slightly positive of the Co^{II}/Co^{I} redox couple results from the protonation of a non-acetate bound Co^{I} species, we sought to determine the effect of electron-withdrawing and -donating groups on the ancillary $PY5Me_2$ ligand on the observed catalysis. The cyclic voltammograms of **1**, $[Co(CF_3PY5Me_2)](OTf)_2$ (**5**), and $[Co(NMe_2PY5Me_2)](OTf)_2$ (**6**) in the presence of 10-fold excesses of various acids having pK_a values[20] ranging from 15.3 to 27.2 are shown in Fig. 10. A number of general trends become apparent. All acids give rise to enhanced currents at the Co^{II}/Co^{I} couple, with the strongest acids resulting in the greatest current enhancements; while not competent acids for efficient H_2 production, even the phenolic acids give slight current enhancements at the Co^{II}/Co^{I} couple. Furthermore, redox events attributable to the anation of all conjugate bases are observable at potentials more negative than the Co^{II}/Co^{I} couple, and current enhancements from the anated Co^{II}/Co^{I} couple are apparent, especially when stronger acids are utilized; anation

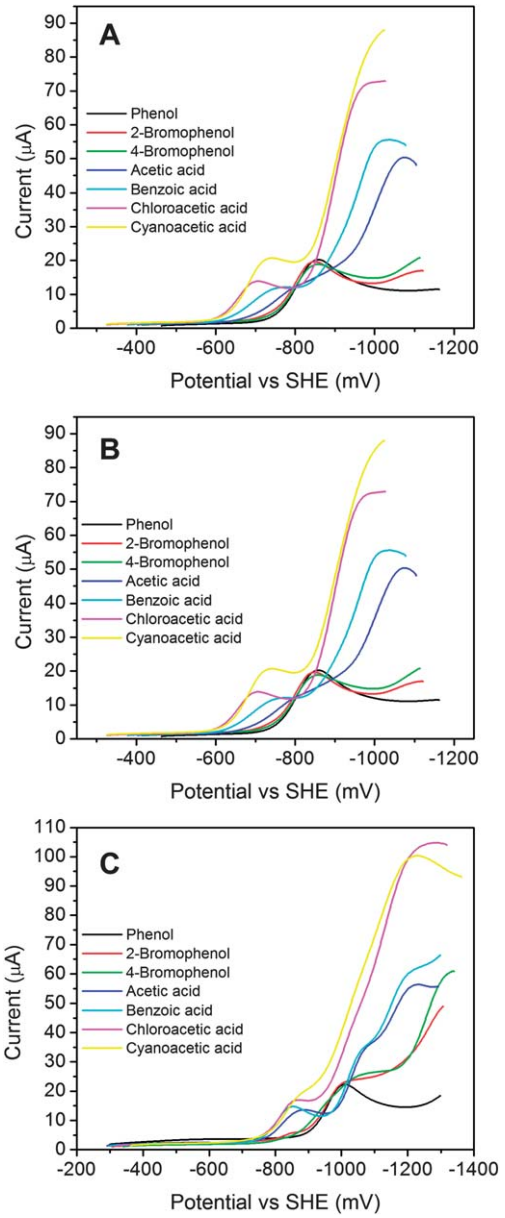

Fig. 10 Cyclic voltammograms of $[Co(X–PY5Me_2)]^{2+}$ (X = H, CF_3, NMe_2) complexes upon addition of various acids. General conditions for all plots: $[Co(X–PY5Me_2)]^{2+}$ = 1 mM, [acid] = 10 mM, $[Bu_4NPF_6]$ = 100 mM, working/auxiliary/reference electrodes = glassy carbon disk/Pt wire/silver wire, scan rate = 100 mV s^{-1}. Acids used are phenol (black), 2-bromophenol (red), 4-bromophenol (green), acetic acid (blue), benzoic acid (aqua), chloroacetic acid (pink), and cyanoacetic acid (yellow). (A) Compound **5**. (B) Compound **1**. (C) Compound **6**.

events are also observed when the phenolic acids are used (Fig. S8†). Catalyst electronics also attenuate the onset of catalysis: the trifluoromethyl derivative requires stronger acids to affect catalysis while catalysis occurs more easily from the dimethylamino derivative.

Reactivity of 3 with tosic acid

Finally, direct protonation studies were undertaken in order to evaluate the competency of **3** with regards to proton reduction in the absence of additional reducing agent. Addition of 1 equivalent of **3** to a large excess of tosic acid results in an extremely rapid color change from dark blue to brown, followed by bleaching over several hours (Fig. S9†). Compound **1** can be recovered from the protonation reaction mixtures; gas chromatography experiments indicate that the protonolysis of **3** with a large excess of tosic acid results in the formation of 0.6 equivalents of H_2 for every two equivalents of **3** used.

Mechanistic considerations

Several mechanisms for the electrocatalytic reduction of protons by Co^{II} species have been proposed in the literature.[15,21] The initial step involves reduction of Co^{II} to Co^{I}; under most experimental conditions the Co^{I} undergoes protonation to yield a $Co^{III}(H)$. In the heterolytic pathway, protonation of the resulting $Co^{III}(H)$ yields H_2 and a Co^{III} species that is readily reduced to a lower oxidation state under the reaction conditions. In the homolytic pathway, a bimolecular reaction involving the $Co^{III}(H)$ species results in H_2 release. In the reduction-protonation pathway, the $Co^{III}(H)$ is further reduced to a $Co^{II}(H)$ species that is subsequently protonated to generate H_2. Finally, a fourth postulated mechanism involves further reduction to a Co^{0} species that reacts rapidly with acid to form a $Co^{II}(H)$ intermediate that immediately precedes H_2 extrusion.

Scheme 2 shows the pathways implicated in electrocatalytic proton reduction using compound **1**. In analogy to previously reported cobalt proton-reduction catalysts, $[Co(PY5Me_2)]^{2+}$ is first reduced to a Co^{I} species as either the solvent- or acetate-bound complex. It is important to note that, while compound **3** was crystallized as a pentacoordinate species from non-coordinating solvent, the formation of an acetonitrile-bound complex of **3** under catalytic conditions cannot be excluded. In both the solvent-bound and anation pathways, protonation of the Co^{I} species is the rate-determining step. The processes occurring after the presumed formation of the Co^{III}-hydride with the pentapyridyl ligand system remain unclear, however, because the system yielded very little information regarding the subsequent steps involved in H_2 evolution. The isolation of a Co^{II} species instead of a Co^{III} species from the protonation of **3** with excess strong acids argues against a heterolytic pathway, and the observation of catalysis at potentials slightly positive of the respective $Co^{II/I}$ couples eliminates a double reduction to Co^{0} under the conditions examined in this study.[21f,g] Distinguishing between a bimolecular decay of a Co^{III}-hydride or the reduction of a Co^{III}-hydride followed by protonation is difficult, however, because the presumed Co^{III}-hydride could not be isolated and subjected to spectroscopic and kinetic studies akin to those recently reported for the $[Co^{I}triphos]^{+}$ system.[21g]

The demonstration that anation is a major factor in proton reduction by the $[Co(PY5Me_2)]^{2+}$ systems has potential implications for other cobalt proton reduction catalysts, most notably in the interpretation of cyclic voltammograms under catalytic conditions that result in the formation of coordinating conjugate bases such as acetate. To the best of our knowledge, only

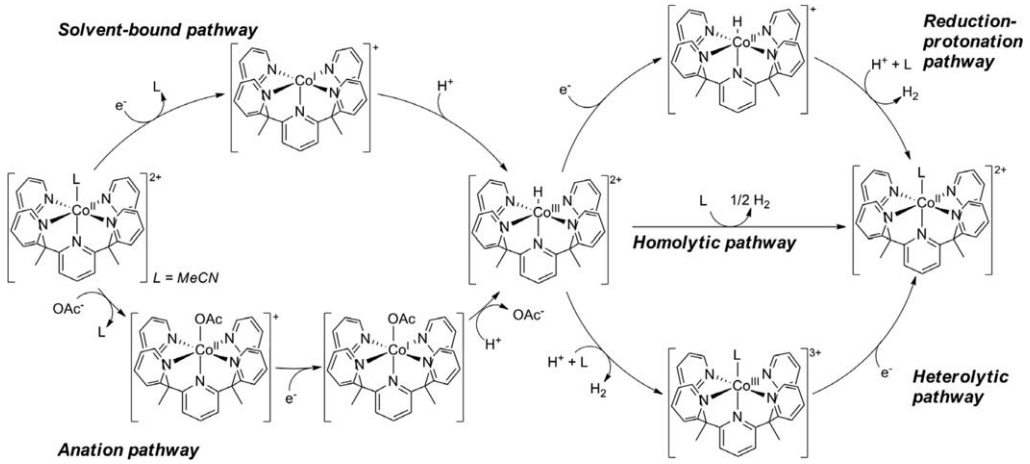

Scheme 2 Mechanistic pathways for proton reduction with compound **3**.

Peters and Hu have identified anation processes operative in cobalt-catalyzed proton reduction systems, with the specific example of proton reduction of hydrochloric acid using a cobalt-diglyoximate catalyst.[7h] While the anation of chloride anions is not surprising, the observation of tosylate anation recently reported by Gray[21g] suggests that anation from more weakly-coordinating anions may also occur under catalytic conditions. Surprisingly, the observation of anation processes resulting from the use of carboxylate and phenolic acids in cobalt-catalyzed proton reduction systems has not been explicitly documented. The use of such common acids has important implications for the mechanism of cobalt-catalyzed proton reductions, and subsequently for the interpretation of cyclic voltammograms. First, use of acetic acid provides an acetate source that is capable of producing a $[Co(PY5Me_2)(OAc)]^+$ species that displays proton reduction at more negative potentials than an acetonitrile-bound complex. After each turnover occurring from the $Co^{II/I}$ couple, one equivalent of acetate is produced. The larger acetate concentration in turn leads not only to a greater concentration of $[Co(PY5Me_2)(OAc)]^+$ but also a larger concentration of free acetate that effectively decreases the concentration of available protons in solution (eqn (4)), thus leading to the slower catalytic turnover that manifests itself as the apparent 'zero-order' dependence in Fig. 3B. The second implication is that anation must be considered in attempting to assign processes in cyclic voltammograms. While computational evidence suggests that the $Co^{II/I}(H)$ redox couple occurs at potentials more negative than the $Co^{II/I}$ couple,[22] experimental assignment of a process as a $Co^{II/I}(H)$ couple requires that anation is eliminated as the potential origin of the new feature.

$$AcOH + AcO^- \rightarrow [AcO–H–OAc]^- \quad (4)$$

A final implication is that the tuning of overpotentials for hydrogen production and other electrocatalytic processes should consider anation in addition to ancillary ligand electronics in order to match appropriate these synergistic redox couples to bond-making and bond-breaking reactions at a given substrate or intermediate. Indeed, the $PY5Me_2$ example in this present study shows that such couples can vary by substantial amounts.

Concluding remarks

The electrochemical and synthetic studies presented here provide additional insight into the mechanisms of proton reduction by the $[Co(PY5Me_2)]^{2+}$ platform. This system represents a rare molecular hydrogen-evolving platform that has been characterized under soluble, diffusion-limited conditions in both organic and aqueous media. In analogy to previously reported mechanisms for proton reduction, the major pathway for H_2 evolution appears to proceed through either the bimolecular decay of the presumed $Co^{III}(H)$ intermediate or further reduction of the $Co^{III}(H)$ to a $Co^{II}(H)$ followed by protonation. A key unique observation made during the course of these studies concerns the extent that anation affects the cyclic voltammogram obtained upon addition of an acid. The coordination of acetate to **1** results in a modulation of the $Co^{II/I}$ redox potential, ultimately resulting in a more electron-rich and thus a more reactive Co^I complex. These data suggest a major mechanistic pathway for aqueous proton reduction by **1** involves a hydroxide- or phosphate-bound catalyst. Indeed, we have previously demonstrated the ability of an aqua ligand to bind to CoPY5 system and that similar cyclic voltammograms are obtained in both aqueous and acetonitrile solvents, suggesting that the observed catalysis after the Co(II)/Co(I) couple in aqueous solution is due to a more negatively charged (*i.e.*, anated) species.[11e,12] More generally, the findings of these studies are expected to have direct implications in the interpretation of other metal-catalyzed proton reduction cycles in the presence of acids with weakly coordinating conjugate bases, but also highlight the broader importance of anation in catalytic processes occurring in aqueous solution. This situation is particularly relevant to proton-coupled electron transfer reactions that lie at the heart of energy-conversion reactions such as proton/water reduction, water oxidation, carbon dioxide fixation, and nitrogen cycling.

Acknowledgements

This research was funded by DOE/LBNL grant 403801 (C.J.C.). The contributions of J.R.L. were supported by NSF Grant CHE-1111900. C.J.C. is an Investigator with the Howard Hughes Medical Institute. Y.S. and N.A.P. acknowledge the Miller Institute for Basic Research for postdoctoral fellowships, and J.P.B. thanks the National Science Foundation for a graduate fellowship.

References

1 (*a*) N. S. Lewis and D. G. Nocera, *Proc. Natl. Acad. Sci. U. S. A.*, 2006, **103**, 15729–15735.

2 (*a*) M. Frey, *ChemBioChem*, 2002, **3**, 153–160; (*b*) D. J. Evans and C. J. Pickett, *Chem. Soc. Rev.*, 2003, **32**, 268–275; (*c*) F. A. Armstrong, *Curr. Opin. Chem. Biol.*, 2004, **8**, 133–140; (*d*) J. A. Turner, *Science*, 2004, **305**, 972–974; (*e*) M. G. Walter, E. L. Warren, J. R. McKone, S. W. Boettcher, Q. Mi, E. A. Santori and N. S. Lewis, *Chem. Rev.*, 2010, **110**, 6446–6473; (*f*) D. G. Nocera, *Acc. Chem. Res.*, 2012, **45**, 767–776; (*g*) C. Herrero, A. Quaranta, W. Leibl, A. W. Rutherford and A. Aukauloo, *Energy Environ. Sci.*, 2011, **4**, 2353–2365; (*h*) W. E. Piers, *Organometallics*, 2011, **30**, 13–16; (*i*) P. Du and R. Eisenberg, *Energy Environ. Sci.*, 2012, **5**, 6012–6021.

3 (*a*) B. E. Barton, M. T. Olsen and T. B. Rauchfuss, *Curr. Opin. Biotechnol.*, 2010, **21**, 292–297; (*b*) P. D. Tran, V. Artero and M. Fontecave, *Energy Environ. Sci.*, 2010, **3**, 727–747.

4 For general reviews, see: (*a*) S. Canaguier, V. Artero and M. Fontecave, *Dalton Trans.*, 2008, **37**, 315–325; (*b*) F. Gloaguen and T. B. Rauchfuss, *Chem. Soc. Rev.*, 2009, **38**, 100–108; (*c*) S. Ogo, *Chem. Commun.*, 2009, **45**, 3317–3325; (*d*) M. Wang, L. Chen, X. Li and L. Sun, *Dalton Trans.*, 2011, **40**, 12793–12800. Specific examples; (*e*) F. Gloaguen, J. D. Lawrence and T. B. Rauchfuss, *J. Am. Chem. Soc.*, 2001, **123**, 9476–9477; (*f*) X. Zhao, I. P. Georgakaki, M. L. Miller, J. C. Yarbrough and M. Y. Darensbourg, *J. Am. Chem. Soc.*, 2001, **123**, 9710–9711; (*g*) F. Gloaguen, J. D. Lawrence, M. Schmidt, S. R. Scott and T. B. Rauchfuss, *J. Am. Chem. Soc.*, 2001, **123**, 12518–12527; (*h*) M. Y. Darensbourg, E. J. Lyon, X. Zhao and I. P. Georgakaki, *Proc. Natl. Acad. Sci. U. S. A.*, 2003, **100**, 3683–3688; (*i*) R. Mejia-Rodriguez, D. Chong, J. H. Reibenspies, M. P. Soriaga and M. Y. Darensbourg, *J. Am. Chem. Soc.*, 2004, **126**, 12004–12014; (*j*) G. A. N. Felton, A. K. Vannucci, J. Chen, L. T. Lockett, N. Okumura, B. J. Petro, U. I. Zakai, D. H. Evans, R. S. Glass and D. L. Lichtenberger, *J. Am. Chem. Soc.*, 2007, **129**, 12521–12530; (*k*) J. Chen, A. K. Vannucci, C. A. Mebi, N. Okumura, S. C. Borowski, M. Swenson, L. T. Lockett, D. H. Evans, R. S. Glass and D. L. Lichtenberger, *Organometallics*, 2010, **29**, 5330–5340; (*l*) D. Chen, R. Scopelliti and X. L. Hu, *Angew. Chem., Int. Ed.*, 2012, **51**, 1919–1921.

5 (*a*) J. O. M. Bockris and B. E. Conway, *Trans. Faraday Soc.*, 1949, **45**, 989–999; (*b*) H. Ezaki, M. Morinaga and S. Watanabe, *Electrochim. Acta*, 1993, **38**, 557–564; (*c*) B. C. H. Steele and A. Heinzel, *Nature*, 2001, **414**, 345–352; (*d*) M. K. Debe, *Nature*, 2012, **486**, 43–51.

6 For general reviews, see: (*a*) V. Artero, M. Chavarot-Kerlidou and M. Fontecave, *Angew. Chem., Int. Ed.*, 2011, **50**, 7238–7266; (*b*) M. Wang, L. Chen and L. Sun, *Energy Environ. Sci.*, 2012, **5**, 6763–6778.

7 Selected nickel catalysts: (*a*) B. J. Fisher and R. Eisenberg, *J. Am. Chem. Soc.*, 1980, **102**, 7361–7363; (*b*) J. P. Collin, A. Jouaiti and J. P. Sauvage, *Inorg. Chem.*, 1988, **27**, 1986–1990; (*c*) A. M. Appel, D. L. DuBois and M. Rakowski DuBois, *J. Am. Chem. Soc.*, 2005, **127**, 12717–12726; (*d*) D. H. Pool and D. L. DuBois, *J. Organomet. Chem.*, 2009, **694**, 2858–2865; (*e*) M. L. Helm, M. P. Stewart, R. M. Bullock, M. R. DuBois and D. L. DuBois, *Science*, 2011, **333**, 863–866; (*f*) D. H. Pool, M. P. Stewart, M. O'Hagan, W. J. Shaw, J. A. S. Roberts, R. M. Bullock and D. L. DuBois, *Proc. Nat. Acad. Sci. U. S. A.*, 2012, **109**, 15634–15639; (*g*) S. E. Smith, J. Y. Yang, D. L. DuBois and R. M. Bullock, *Angew. Chem., Int. Ed.*, 2012, **51**, 3152–3155. Iron catalysts: See ref. 4f as a leading reference.; (*h*) Selected cobalt catalysts: X. L. Hu, B. M. Cossairt, B. S. Brunschwig, N. S. Lewis and J. C. Peters, *Chem. Commun.*, 2005, **37**, 4723–4725; (*i*) G. M. Jacobsen, J. Y. Yang, B. Twamley, A. D. Wilson, R. M. Bullock, M. R. DuBois and D. L. DuBois, *Energy Environ. Sci.*, 2008, **1**, 167–174; (*j*) L. A. Berben and J. C. Peters, *Chem. Commun.*, 2010, **46**, 398–400; (*k*) E. S. Wiedner, J. Y. Yang, W. G. Dougherty, W. S. Kassel, R. M. Bullock, M. R. DuBois and D. L. DuBois, *Organometallics*, 2010, **29**, 5390–5401; (*l*) W. R. McNamara, Z. Han, P. J. Alperin, W. W. Brennessel, P. L. Holland and R. Eisenberg, *J. Am. Chem. Soc.*, 2011, **133**, 15368–15371; (*m*) W. R. McNamara, Z. Han, C.-J. Yin, W. W. Brennessel, P. L. Holland and R. Eisenberg, *Proc. Natl. Acad. Sci. U. S. A.*, 2012, **109**, 15594–15599; (*n*) W. M. Singh, T. Baine, S. Kudo, S. Tian, X. A. N. Ma, H. Zhou, N. J. DeYonker, T. C. Pham, J. C. Bollinger, D. L. Baker, B. Yan, C. E. Webster and X. Zhao, *Angew. Chem., Int. Ed.*, 2012, **51**, 5941–5944.

8 (*a*) For a general review of tethered or adsorbed molecular catalysts, see J. L. Inglis, B. J. MacLean, M. T. Pryce and J. G. Vos, *Coord. Chem. Rev.*, 2012, **256**, 2571–2600.; (*b*) For specific examples of aqueous-compatible systems containing either tethered or adsorbed molecular systems, see the following: A. Le Goff, V. Artero, B. Jousselme, P. D. Tran, N. Guillet, R. Metaye, A. Fihri, S. Palacin and M. Fontecave, *Science*, 2009, **326**, 1384–1387; (*c*) E. S Andreiadis, P.-A. Jacques, P. D. Tran, A. Leyris, M. Chavarot-Kerlidou, B. Jousselme, M. Matheron, J. Pecaut, S. Palacin, M. Fontecave and V. Artero, *Nat. Chem.*, 2012, **5**, 48–53; (*d*) M. Guttentag, A. Rodenberg, C. Bachmann, A. Senn, P. Hamm and R. Alberto, *Dalton Trans.*, 2013, **42**, 334–337.

9 (*a*) H.-Y. Wang, W.-G. Wang, G. Si, F. Wang, C.-H. Tung and L.-Z. Wu, *Langmuir*, 2010, **26**, 9766–9771; (*b*) U. J. Kilgore, J. A. S. Roberts, D. H. Pool, A. M. Appel, M. P. Stewart, M. R. DuBois, W. G. Dougherty, W. S. Kassel, R. M. Bullock and D. L. DuBois, *J. Am. Chem. Soc.*, 2011, **133**, 5861–5872;

(*c*) C. C. L. McCrory, C. Uyeda and J. C. Peters, *J. Am. Chem. Soc.*, 2012, **134**, 3164–3170; (*d*) F. Quentel, G. Passard and F. Gloaguen, *Energy Environ. Sci.*, 2012, **5**, 7757–7761.

10 V. S. Thoi, Y. Sun, J. R. Long and C. J. Chang, *Chem. Soc. Rev.*, 2013, DOI: 10.1039/c2cs35272a.

11 (*a*) H. I. Karunadasa, C. J. Chang and J. R. Long, *Nature*, 2010, **464**, 1329–1333; (*b*) V. S. Thoi, H. I. Karunadasa, Y. Surendranath, J. R. Long and C. J. Chang, *Energy Environ. Sci.*, 2012, **5**, 7762–7770; (*c*) H. I. Karunadasa, E. Montalvo, Y. Sun, M. Majda, J. R. Long and C. J. Chang, *Science*, 2012, **335**, 698–702; (*d*) J. P. Bigi, T. E. Hanna, W. H. Harman, A. Chang and C. J. Chang, *Chem. Commun.*, 2010, **46**, 958–960; (*e*) Y. Sun, J. P. Bigi, N. A. Piro, M. L. Tang, J. R. Long and C. J. Chang, *J. Am. Chem. Soc.*, 2011, **133**, 9212–9215.

12 Y. Sun, J. Sun, J. R. Long, P. Yang and C. J. Chang, *Chem. Sci.*, 2013, **4**, 118–124.

13 (*a*) V. Houlding, T. Geiger, U. Kölle and M. Grätzel, *J. Chem. Soc., Chem. Commun.*, 1982, 681–683; (*b*) R. M. Kellett and T. G. Spiro, *Inorg. Chem.*, 1985, **24**, 2373–2377; (*c*) U. Koelle and S. Paul, *Inorg. Chem.*, 1986, **25**, 2689–2694; (*d*) R. Abdel-Hamid, H. M. El-Sagher, A. M. Abdel-Mawgoud and A. Nafady, *Polyhedron*, 1998, **17**, 4535–4541; (*e*) P. V. Bernhardt and L. A. Jones, *Inorg. Chem.*, 1999, **38**, 5086–5090.

14 J. Shearer, I. Y. Kung, S. Lovell, W. Kaminsky and J. A. Kovacs, *J. Am. Chem. Soc.*, 2001, **123**, 463–468.

15 X. Hu, B. S. Brunschwig and J. C. Peters, *J. Am. Chem. Soc.*, 2007, **129**, 8988–8998.

16 (*a*) D. H. Pool and D. L. DuBois, *J. Organomet. Chem.*, 2009, **694**, 2858–2865; (*b*) U. J. Kilgore, J. A. S. Roberts, D. H. Pool, A. M. Appel, M. P. Stewart, M. R. DuBois, W. G. Dougherty, W. S. Kassel, R. M. Bullock and D. L. DuBois, *J. Am. Chem. Soc.*, 2011, **133**, 5861–5872.

17 B. D. Stubbert, J. C. Peters and H. B. Gray, *J. Am. Chem. Soc.*, 2011, **133**, 18070–18073.

18 (*a*) O. Pantani, S. Naskar, R. Guillot, P. Millet, E. Anxolabéhére-Mallart and A. Aukauloo, *Angew. Chem., Int. Ed.*, 2008, **120**, 9948; (*b*) Y. Z. Voloshin, A. V. Dolganov, O. A. Varzatskii and Y. N. Bubnov, *Chem. Commun.*, 2011, **47**, 7737.

19 E. Anxolabéhére-Mallart, C. Costentin, M. Fournier, S. Nowak, M. Robert and J.-M. Savéant, *J. Am. Chem. Soc.*, 2012, **134**, 6104–6107.

20 pK_a values obtained from G. A. N. Felton, R. S. Glass, D. L. Lichtenberger and D. H. Evans, *Inorg. Chem.*, 2006, **45**, 9181–9184.

21 (*a*) For a general review, see J. L. Dempsey, B. S. Brunschwig, J. R. Winkler and H. B. Gray, *Acc. Chem. Res.*, 2009, **42**, 1995–2004. For specific studies see; (*b*) P. Connolly and J. H. Espenson, *Inorg. Chem.*, 1986, **25**, 2684–2688; (*c*) C. Baffert, V. Artero and M. Fontecave, *Inorg. Chem.*, 2007, **46**, 1817–1824; (*d*) J. L. Dempsey, J. R. Winkler and H. B. Gray, *J. Am. Chem. Soc.*, 2010, **132**, 16774–16776; (*e*) J. L. Dempsey, J. R. Winkler and H. B. Gray, *J. Am. Chem. Soc.*, 2010, **132**, 1060–1065; (*f*) C. H. Lee, D. K. Dogutan and D. G. Nocera, *J. Am. Chem. Soc.*, 2011, **133**, 8775–8777; (*g*) S. C. Marinescu, J. R. Winkler and H. B. Gray, *Proc. Natl. Acad. Sci. U. S. A.*, 2012, **109**, 15127–15131.

22 (*a*) J. T. Muckerman and E. Fujita, *Chem. Commun.*, 2011, **47**, 12456–12458; (*b*) B. H. Solis and S. Hammes-Schiffer, *Inorg. Chem.*, 2011, **50**, 11252–11262; (*c*) B. H. Solis and S. Hammes-Schiffer, *J. Am. Chem. Soc.*, 2011, **133**, 19036–19039.